Sterically and Guest-Controlled Self-Assembly of Calix[4]arene Derivatives

Alexander Shivanyuk,*[a, d] Mohamed Saadioui,[b] Frank Broda,[c] Iris Thondorf,*[c] Myroslav O. Vysotsky,[b] Kari Rissanen,[a] Erkki Kolehmainen,[a] and Volker Böhmer*[b]

Dedicated to Professor Julius Rebek Jr. on the occasion of his 60th birthday

Abstract: In solvents such as chloroform or benzene, tetraurea calix[4]arenes **1** form dimeric capsules in which one solvent molecule is usually included as guest. To explore the structural requirements for the formation of such hydrogen-bonded dimers we replaced one *p*-tolylurea residue by a simple acetamide function. The resulting calix[4]arene **2a**, substituted at its wide rim with one acetamide and three *p*-tolylurea functions, assumes a C_1-symmetrical conformation in apolar solvents as shown by ^{1}H NMR, which is not compatible with the usual capsule. In the crystalline state, four molecules of **2a**, adopting a pinched cone conformation, assemble into a quasi S_4-symmetrical tetramer stabilized by a cyclic array of 24 NH···O=C hydrogen bonds and four NH···π interactions. Four acetamide groups are hydrogen-bonded to each other and pack tightly in the center of the assembly. All polar residues are buried inside the tetramer, the surface of which is lipophilic. Extensive NMR studies revealed similar structures in apolar solvents such as [D]chloroform or [D_6]benzene for calixacetamides **2a–c.** The formation of these tetramers in solution is critically dependent on the size of the amide fragment, so that propionamide **2d**, butyramide **2e**, and *p*-tolylamide **2f** form only ill-defined aggregates. This is caused by steric crowding inside the tetrameric assembly. The tetramers persist during molecular dynamics simulations, and the optimized average structure of the MD run is similar to that found in the crystalline state. Theoretical studies revealed that cooperation of hydrogen bonds with multiple NH···π, C–H···π, and π···π attractions make the tetramer more stable than the capsular dimer with the solvent as guest. In the presence of tetraethylammonium salts, however, compounds **2a–e** form dimeric capsular assemblies, each incorporating a single ammonium cation. Only one of two possible regioisomeric dimers is formed, in which both acetamide groups are surrounded by two urea residues. These examples give striking evidence of how self-assembly in solution can be strongly dependent on subtle structural factors and of how the formation of dimeric capsules can be induced by the presence of an appropriate guest.

Keywords: calixarenes · hydrogen bonds · self-assembly · supramolecular chemistry

Introduction

Calix[4]arene tetraurea derivatives of type **1** (Figure 1) have been shown to form hydrogen-bonded dimeric capsules[1] capable of reversible encapsulation of neutral and cationic

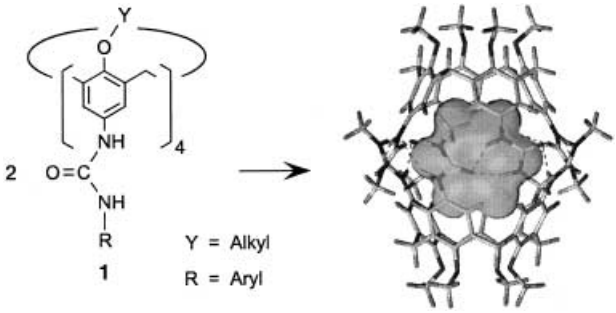

Figure 1. Tetraurea calix[4]arene **1** and its dimeric capsule (R = Y = CH_3) in stick presentation.

[a] Dr. A. Shivanyuk, Prof. K. Rissanen, Prof. E. Kolehmainen
NanoScience Center, Department of Chemistry,
University of Jyväskylä
P.O. Box 35, FIN-40351, Jyväskylä (Finland)
E-mail: Kari.Rissanen@jyu.fi

[b] Dr. M. Saadioui, Dr. M. O. Vysotsky, Dr. V. Böhmer
Fachbereich Chemie und Pharmazie, Abteilung Lehramt Chemie
Johannes Gutenberg-Universität, Duesbergweg 10–14,
55099 Mainz (Germany)
E-mail: vboehmer@mail.uni-mainz.de

[c] F. Broda, PD Dr. I. Thondorf
Fachbereich Biochemie/Biotechnologie, Institut für Biochemie
Martin-Luther-Universität Halle-Wittenberg,
Kurt-Mothes-Strasse 3, 06099 Halle (Germany)
E-mail: thondorf@biochemtech.uni-halle.de

[d] Dr. A. Shivanyuk
Current address:
Institute of Organic Chemistry
National Academy of Sciences of Ukraine
Murmanskaya Street 5, Kiev, 02066 (Ukraine)
E-mail: shivangg@netscape.net

DOI: 10.1002/chem.200305633

guests in non-polar media. The two calix[4]arene moieties are held together by a seam of 16 NH···O=C hydrogen bonds between the (interdigitating) urea residues. ^{1}H NMR spectra suggested a stronger hydrogen bond for NH_α (attached to R) than for NH_β (attached to the calixarene), which was confirmed for capsules with benzene as guest by a shorter N···O distance in the crystalline state.[2] Inclusion of the larger tetraethylammonium cation leads to an expansion of the capsule, with only eight hydrogen bonds—mainly of the NH_α···O=C type—now being found in the crystal.[3] Modifications of the ether residues Y at the narrow rim and/or the urea functions at the wide rim resulted in various supramolecular assemblies, including capsular polymers (polycaps),[4] chiral capsules,[5] and a unimolecular capsule.[6] The introduction of bulky urea residues R led to dimeric capsules with outstanding kinetic stabilities.[7] These have been shown to decompose slowly on the human timescale even in polar solvents such as DMSO.[8]

Hydrogen-bonded, dimeric capsules also have been reported for tetra-ureidopeptide derivatives of calix[4]arenes,[9] in which two hydrogen bond arrays are superimposed, and for alanine-substituted derivatives.[10] Dimeric capsules are also formed from calix[4]arenes with oppositely charged functional groups at the wide rim.[11]

Structural modifications of the urea functions may be used to obtain further insight into the factors determining the stability of the hydrogen-bonded dimer. A serendipitous discovery of such a modification was the observation that tetratosyl- and tetraaryl-ureas prefer to form heterodimers when mixed.[12] We were interested in whether all four urea residues are necessary to form a stable capsule, and replaced one urea group by a simple amide group, thus eliminating one of the NH_α groups. While these triurea monoamides form the usual capsules when ammonium cations are offered as guest, this structural modification completely changes the assembly formed in aprotic solvents which are usually included as guest. We have discovered that calix[4]arene triurea monoacetamides **2a** and **2b** (Scheme 1) form hydrogen-bonded tetramers composed of calix[4]arenes in a strongly pinched cone conformation in the crystalline state and in non-polar solvents.

Results and Discussion

Synthesis: Treatment of tetraamine **3** with one equivalent of *tert*-butyloxycarbonyl (Boc) anhydride gave the mono-Boc-protected compound **4** (Scheme 1).[13] Acylation with isocyanates afforded the triureas **5**, which were then deprotected with trifluoroacetic acid (TFA) to give the amines **6** as triflate salts. Finally, acylation of **6** with acid anhydrides or acid chlorides yielded compounds **2**, each bearing three urea functions and one amide moiety at its wide rim.

Single-crystal X-ray analysis: Slow crystallization of monoacetamide **2a** from a three-component mixture (MeCN/CH_2Cl_2/H_2O) afforded colorless transparent crystals, which, although unstable in the absence of mother liquor, were suitable for single-crystal X-ray analysis.

In the crystalline state, a molecule of **2a** adopts a pinched cone conformation[14] (Figure 2a) in which the calixarene aryl ring **A** bearing the acetamide fragment is strongly bent

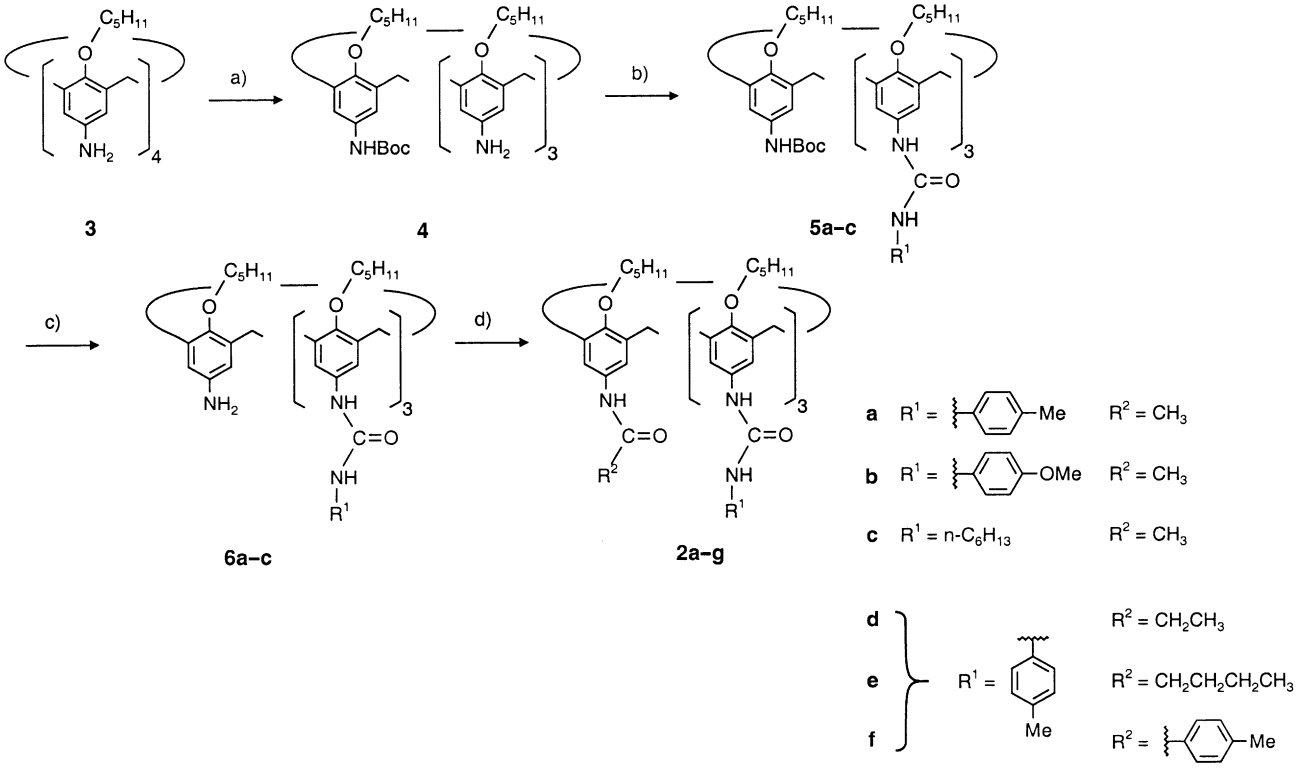

Scheme 1. a) Boc_2O, $CHCl_3$, RT; b) R^1NCO, THF, RT; c) TFA, CH_2Cl_2, RT; d) R^2COCl or $(R^2COO)_2$, RT.

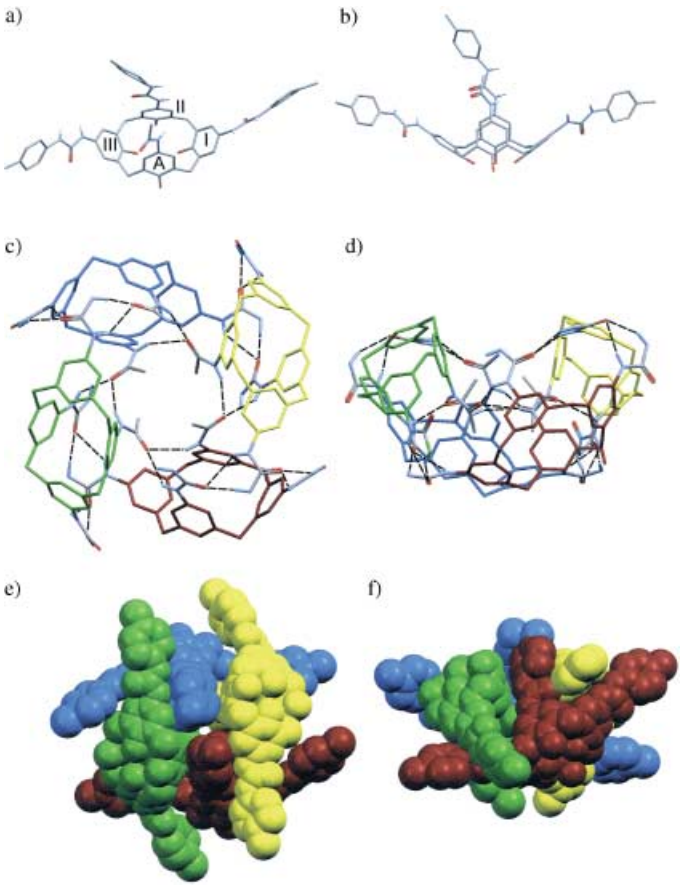

Figure 2. Single-crystal X-ray structure of $\mathbf{2a}_4$: a, b) Conformation of a single molecule of **2a** seen from two directions (only NH hydrogen atoms are shown, while pentyl groups are omitted for clarity). c, d) Stick presentation of the tetrameric assembly of **2a** (pendant pentoxy chains and *para*-tolyl fragments are omitted for clarity; hydrogen bonds are shown in dashed lines); the S_4 axis is perpendicular to the drawing plane in (c) and the orientation shown in (d) is obtained by a 90° rotation around a horizontal axis. e, f) Space-filling representation of the complete tetramer $\mathbf{2a}_4$ (pentyl chains are omitted, orientations are similar to those in (c,d)).

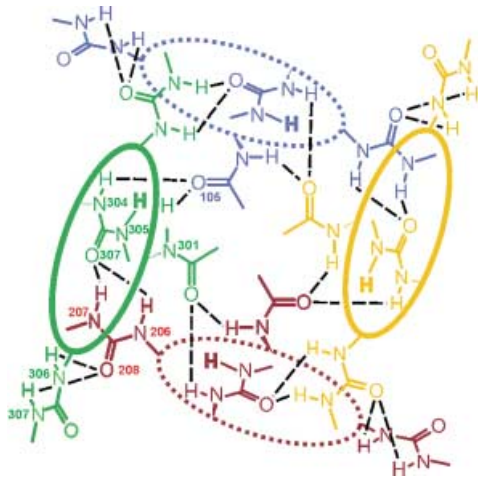

Figure 3. Schematic drawing of the hydrogen bonding pattern found in the crystal structure of $\mathbf{2a}_4$. Ellipses denote the wider rim of the calixarene subunits; they are drawn in bold lines when they lie above the plane of the acetamide carbonyl groups (with their substituents pointing away from the viewer), while dashed lines indicate that they are below this area and the substituents are pointing upwards. Hydrogen bonds are represented with dashed bold black lines. Hydrogens involved in NH···π interactions are typed bold. Only atoms mentioned in Table 3 are marked.

towards the opposite ring **II** bearing the *p*-tolylurea fragment (dihedral angle −24.9 to −26.0° for the four calix[4]arenes in the tetramer; see below). The dihedral angle between the other two aryl rings **I** and **III** is 107–110.3°. The aromatic rings form the following dihedral angles with the best plane through the methylene bridge carbons: **A**: 72.1–72.5°, **I**: 143.0–145.6°, **II**: 81.6–83.0°, and **III**: 144.0–145.3°. The pendant amide groups are oriented in a chiral, C_1-symmetrical (Figure 2a) manner such that the carbonyl groups of three urea fragments are pointing clockwise (or counterclockwise), while the carbonyl of the acetamide is pointing counterclockwise (or clockwise). No intramolecular hydrogen bonds are found between the amide groups at the wide rim of the calixarene.

Two pairs of enantiomers of **2a** form a cyclic, hydrogen-bonded tetramer of somewhat distorted S_4 symmetry (Figure 2b, Figure 3). The conformations of these four molecules and their intermolecular distances are hence slightly different. For each distance, angle, etc. an average of the four values is given below. The four acetamide groups are positioned in the middle of the assembly, connected through a cycle of four NH···O=C hydrogen bonds (N−O distances 2.95 Å). Each amide carbonyl oxygen accepts a second hydrogen bond from the calix-attached urea NH_β of ring **II** in the adjacent calixarene (N−O distance 2.95 Å), while its tolyl-attached urea NH_α forms NH···π contacts (3.66 Å) with the aryl ring **A**. Three-centered hydrogen bonds connect the carbonyl oxygen of ring **II** with both NH groups of ring **III** in a third calixarene and its carbonyl oxygen with both NH groups of ring **I** in the second calixarene. The carbonyl oxygen at ring **I** is not involved in hydrogen bonding. In this sequence the hydrogen bonds of NH_β groups connected to the *p*-tolyl fragments are considerably shorter (N−O distances 2.84 and 2.98 Å) than those of NH_α groups attached to the calixarene (N−O distances 3.29 and 3.12 Å).

The tetrameric assembly of **2a** is thus stabilized by 24 NH···O=C hydrogen bonds and four NH···π attractions. As shown in Figure 2c, the cyclic array of the acetamide groups is buried inside the assembly and is shielded by two *p*-tolyl rings of the urea fragments. The shortest distances between the acetamide methyl groups is 4.3 Å, suggesting that the tetramer formation must be critically dependent on the size of the amide fragment.

No strong interactions between adjacent tetramers were found. Because of the irregular shape of $\mathbf{2a}_4$, the crystal contains channels filled with disordered dichloromethane, acetonitrile, and water molecules. Further disorder of many pentyl chains causes the high final *R* values of the structure.

Solution studies: The ^{1}H NMR spectrum of **2a** in [D_6]DMSO or [D_6]acetone contains two *meta*-coupled doublets and two singlets for the calixarene aromatic protons and two pairs of doublets for the methylene bridges. Two

sets of signals in 2:1 ratio are observed for the C–H and NH_α protons of the *p*-tolyl urea fragments. The NH and CH_3 protons of the acetamide group emerge as singlets at $\delta = 9.47$ and 2.21 ppm, respectively. Analogous spectra are observed for **2b–f**. Their NMR patterns are consistent with a time-averaged C_s-symmetrical structure, as would be expected for the monomeric calix[4]arenes.

Twenty-one ^{1}H NMR signals are observed for the NH and the aromatic protons of **2a** (Figure 4a,c) in nonpolar solvents such as [D]chloroform or [D_6]benzene. The 2D COSY and ^{1}H–^{13}C HMBC spectra show that eight *meta*-coupled doublets ($J = 2.0$ Hz) correspond to the aromatic protons of calixarene rings while the protons of the tolyl fragments emerge as six doublets with $J = 8.0$ Hz. The remaining seven singlets correspond to the NH protons of the urea and acetamide residues. In the aliphatic region, eight doublets are found for the methylene bridges, together with three singlets in 1:1:1 ratio for the tolyl methyl protons (Figure 4b). One sharp signal for the methyl protons of the acetamide fragment is positioned at $\delta = 1.33$ ppm, which is shifted upfield by 0.89 ppm relative to the same signal in [D_6]DMSO. We therefore observe a single calixarene conformation with C_1 symmetry and stable on the NMR time scale.

In [D]chloroform, six ^{15}N NMR doublets were identified by ^{1}H–^{15}N HMBC spectroscopy for the nitrogen atoms of the urea fragments, between $\delta = -279.3$ and -274.0 ppm, unlike in [D_6]DMSO, in which only two overlapping peaks could be detected, at $\delta = -274.8$ and -275.1 ppm. The resonances of N3, N4, and N7 show cross-peaks to the ^{1}H NMR signals of the *ortho*-protons of the *p*-tolyl fragments, whereas N2, N5, and N6 correlate with the aromatic protons of the calixarene skeleton (Figure 4c). NOESY correlations allowed assignment of the NH signals in the same urea residue. The ^{15}N NMR resonance for the acetamide group (N1) appears at $\delta = -245.1$ ppm and gives cross-peaks to the ^{1}H NMR signals of the NH proton (H2), the methyl group of the acetamide fragment (H33), and one *meta*-coupled doublet of aromatic calixarene protons (H19). The COSY spectrum shows that H19 is coupled with H16. In turn, H16 gives a NOESY cross-peak to H5, and both H5 and H16 correlate with the closest methylene protons of the bridges. All the protons of the aromatic rings, NH groups, and methylene bridges were identified by this methodology. The resonances of the methyl groups of the *p*-tolyl fragments were assigned through NOEs to the *ortho*-protons, which were in turn established from the ^{1}H–^{15}N HMBC and COSY experiments. The intensities of the NOEs between the aromatic protons of the calixarene and the closest NH protons reveal that the arrangement of the urea and acetamide groups of **2a** in [D]chloroform is the same as in the crystal structure of $\mathbf{2a}_4$ (Figure 2a, Figure 4c).

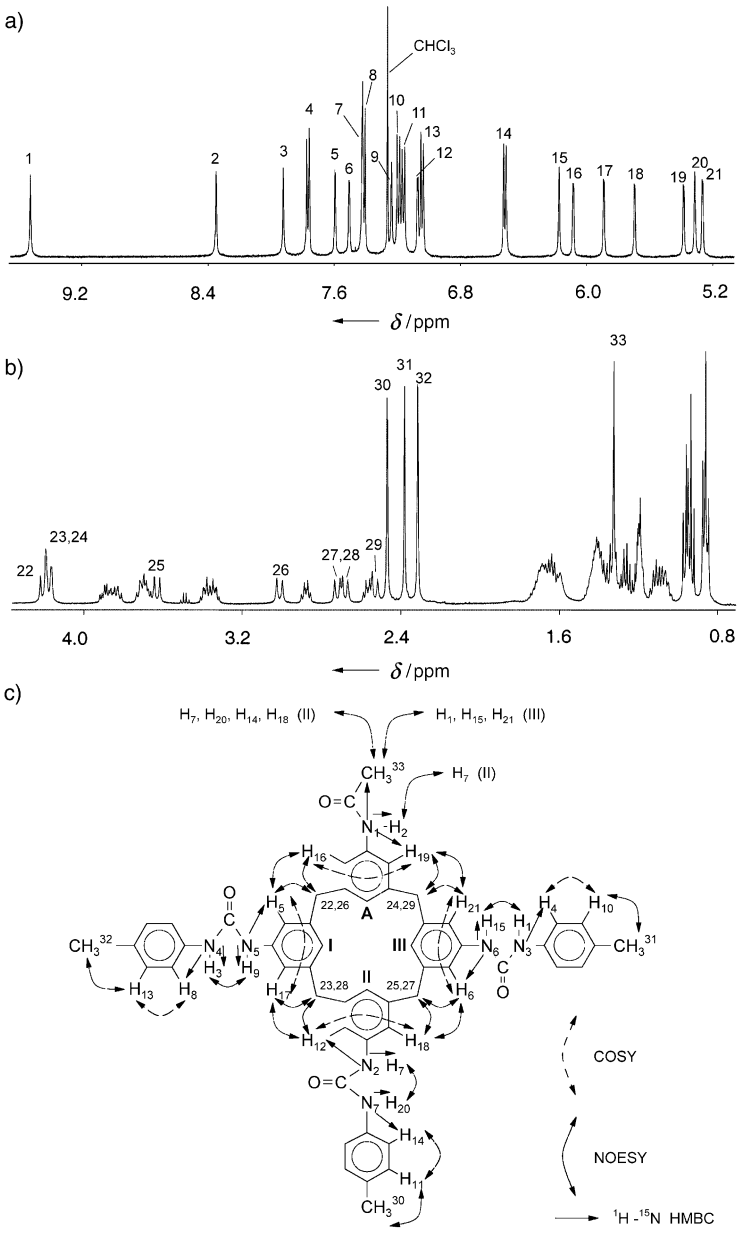

Figure 4. ^{1}H NMR spectrum of **2a** in [D]chloroform (500 MHz, [**2a**] = 5 mM, 303 K): a) aromatic and NH signals, b) aliphatic signals, c) assignment of the peaks. The NOESY correlations H^2–H^{19}, H^{15}–H^{21}, H^7–H^{18}, H^9–H^{17} are omitted for clarity.

Further evidence of the tetrameric structure of **2a** in [D]chloroform came from dynamic NOE studies.[15] The saturation of one equatorial proton at different mixing times results in a NOE with the corresponding axial proton.[16] The linear part of the NOE-buildup curves allowed the evaluation of cross-relaxation constants (σ_{IS}), which are related to the molecular size. In the case of *tert*-butylcalix[4]arene tetrapentyl ether, the NOEs are *positive* with $\sigma_{IS} = 0.33\ s^{-1}$. An analogous experiment with the dimer $\mathbf{1}_2$ (Y = C_5H_{11}, R = *p*-tolyl; see Figure 1) gives *negative* NOEs with $\sigma_{IS} = -0.70\ s^{-1}$, due to slower tumbling of the dimeric capsule $\mathbf{1}_2$. The aggregate of acetamide **2a** is about twice as large as $\mathbf{1}_2$, as indicated by $\sigma_{IS} = -1.70\ s^{-1}$.

In principle, the observation of a single C_1-symmetrical calix[4]arene could be explained by a tetrameric assembly with C_4, D_2, or S_4 symmetry. Intermolecular cross-peaks found in the NOESY and ROESY spectra are entirely consistent with a time-averaged S_4 symmetry as found in the X-ray structure.

The nature of the urea fragments in **2a** is not decisive for its tetramerization, since compounds **2b** and **2c** also form tetrameric assemblies in [D]chloroform. The tetramerization of **2a–c** also occurs in [D_2]dichloromethane, [D_6]benzene, and [D_8]toluene. No other species can be observed by ^{1}H NMR down to concentrations of 1×10^{-4} M. No significant changes in the NMR spectra were observed in chloroform between 223 and 328 K and in [D_{10}]xylene between 298 and 383 K, suggesting stability of the tetramer over this temperature range. Vapor pressure osmometry (VPO) of **2a** in benzene gave an aggregation number of 3.8, in reasonable agreement with the existence of tetramers.

In contrast, the propionamide **2d**, butyramide **2e**, and *p*-tolylamide **2f** exist in nonpolar solvents as ill-defined hydrogen-bonded aggregates with very broad NMR spectra. This could be explained in terms of a steric effect of the larger amide residues that should, in accordance with the crystal structure of $\mathbf{2a}_4$, prevent the formation of the tetrameric assembly. Acetamides **2a–c** do not form heteroaggregates when mixed with tetraurea **1** in [D]chloroform. Mixing of **2a** and **2b** in a 1:1 ratio results in a very complicated ^{1}H NMR spectrum, most probably reflecting the formation of several heterotetramers in addition to the two homotetramers.

Dimeric capsular complexes with tetraethylammonium salts: When tetraethylammonium bromide or hexafluorophosphate (1.05 mol) is dissolved in a chloroform solution of **2a** (2 mol), drastic changes in the ^{1}H NMR spectrum are observed at 295 K (Figure 5a). A broad resonance at −1.7 ppm is observed for the methyl protons of the Et_4N^+ ion, a value typically found for the inclusion of Et_4N^+ ions in dimers of the tetraureas **1**.[17] The number of signals also corresponds to a dimeric capsule, which is further confirmed by heterodimerization experiments (see below). The observed C_2 symmetry is due to the fast reorientation of the hydrogen-bonded belt. The NMR pattern further manifests the presence of *only one* of two possible regioisomeric capsules. Analogous ^{1}H NMR spectra were observed for the triurea monoamides **2c–e**, indicating that the size of the amide group has no influence on the formation of the dimeric capsules with Et_4N^+ ions, in contrast to the tetrameric assembly described above.

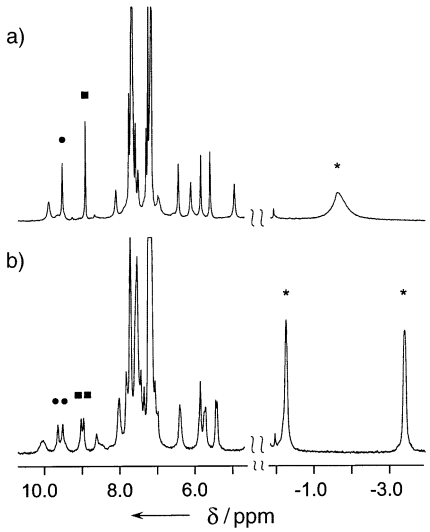

Figure 5. ^{1}H NMR spectra of the dimeric capsule $Et_4N^+\cdot\mathbf{2a}_2\cdot PF_6^-$ (400 MHz, [D]chloroform): a) at 298 K, b) at 223 K. NH protons (marked by ● and ■) are split, due to the slow reorientation of the hydrogen-bonded belt; methyl protons of the encapsulated Et_4N^+ (marked by *) are split due to the slow tumbling of the guest around a pseudo-C_2 axis.

The splitting of the signals for the aromatic and the NH groups at 223 K (Figure 5b) demonstrates that the reorientation of the hydrogen-bonded amide groups (Process I, Figure 6) becomes slow on the NMR time scale. Coalescence temperature analysis gave a $\Delta G^{\neq}$ value of

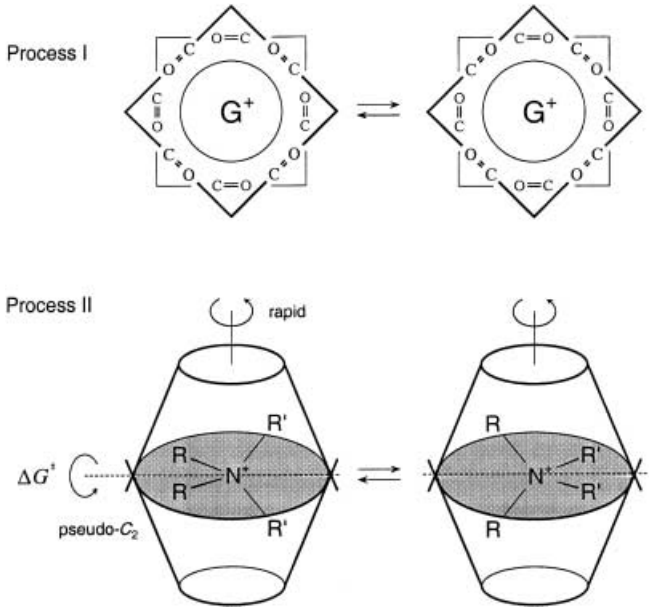

Figure 6. Two different dynamic processes within dimeric capsules of calix[4]arene ureas with Et_4N^+ as guest: reorientation of the hydrogen-bonded belt (Process I) and hindered rotation of the encapsulated Et_4N^+ cation (Process II).

11.2 kcal mol^{-1} (T_c = 225 K), which is somewhat lower than the barrier for $Et_4N^+ \cdot \mathbf{1}_2 \cdot PF_6^-$ ($\Delta G^{\neq}$ = 11.9 kcal mol^{-1} at T_c = 276 K). A decrease in the temperature to 223 K also slows the tumbling of the encapsulated cation (Process II, Figure 6). As a result, the broad resonance at $\delta = -1.7$ ppm (Figure 5a) splits into two signals at $\delta = -0.2$ and -3.4 ppm (Figure 5b). The former corresponds to a pair of guest methyl groups pointing towards the hydrogen-bonded belt, while the latter represent a strong shielding of the methyl groups pointing towards calixarene aromatic rings. Activation barriers of 11.5 kcal mol^{-1} were found for both **2a** and **2c** at coalescence temperatures of 274 and 270 K, respectively. This is significantly lower than for the complex $Et_4N^+ \cdot \mathbf{1}_2 \cdot PF_6^-$ ($\Delta G^{\neq}$ = 13.1 kcal mol^{-1}, T_c = 306 K), indicating a higher mobility of the included guest within the capsule.

To find out which of the two regioisomeric dimers is actually formed we performed a series of NOESY, TOCSY, and COSY experiments for $Et_4N^+ \cdot \mathbf{2a}_2 \cdot Br^-$ and $Et_4N^+ \cdot \mathbf{2d}_2 \cdot Br^-$ at room temperature. Four pairs of *meta*-coupled doublets for the calixarene aromatic protons, three pairs of *ortho*-coupled doublets for the tolyl aromatic protons, and four pairs of doublets for the methylene bridges were assigned by the 2D COSY technique. Additional TOCSY cross-peaks between the signals of NH and aromatic protons were used to assign the amide and the three urea moieties. The connectivity of these moieties within one calix[4]arene molecule was then established from cross-relaxation NOESY peaks. The four cross-peaks between residues **A** and **II** establish the structure of the distal regioisomer (Figure 7, left), while one cross-peak observed between **A** and **III** is possible for both. The absence of close contacts between **I** and **III**, which would be characteristic for the proximal regioisomer, further indicates the exclusive formation of the distal regioisomer.

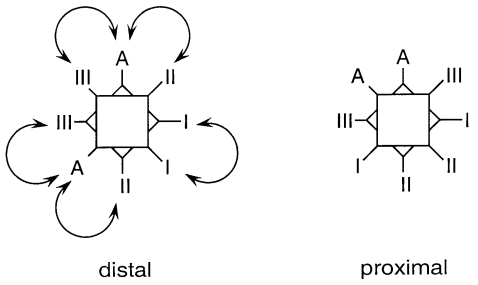

Figure 7. Schematic representation of the two regioisomeric dimers that could be formed by **2**. The aromatic rings bearing acetamide and the three tolyl urea moieties are named **A** and **I**–**III**, respectively. The arrows indicate NOESY correlations.

Amides **2a** and **2d** form a single heterodimer $Et_4N^+ \cdot \mathbf{2a} \cdot \mathbf{2d} \cdot Br^-$ that coexists with the two homodimers**.** The number of signals in the ^{1}H NMR spectrum of the heterodimer (Figure 8a) is in agreement with the expected C_1 symmetry. It seems plausible that the heterodimer has a distal disposition of two different amide groups, similarly to the homodimers. Monoacetamide **2a** and tetraurea **1** also produce a heterodimer in the presence of $Et_4N^+ \cdot Br^-$. The strongest hydrogen-bonded urea NH protons of the heterodimer emerge as four singlets in 1:2:2:2 ratio (Figure 8b), in accordance with the C_s-symmetrical structure.

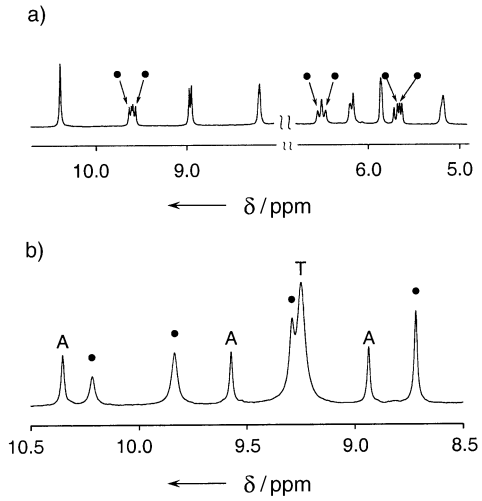

Figure 8. Low-field window of the ^{1}H NMR spectra (400 MHz, [D]chloroform, 298 K) of: a) **2a** + **2d** + $Et_4N^+ \cdot Br^-$, and b) **2a** + **1** + $Et_4N^+ \cdot Br^-$ (peaks for the heterodimers are marked by filled circles (●); peaks for the homodimers $Et_4N^+ \cdot \mathbf{1}_2 \cdot Br^-$ and $Et_4N^+ \cdot \mathbf{2a}_2 \cdot Br^-$ are indicated by **T** and **A**, respectively).

Halide anions can be hydrogen-bonded to calix[4]arenes bearing urea functions at the wide rim.[18] The formation of $Et_4N^+ \cdot \mathbf{2a}_2 \cdot Br^-$ is more favorable when stoichiometric amounts of the guest are used. In the presence of a 1.5-fold excess of $Et_4N^+ \cdot Br^-$ some additional peaks appear (Figure 9a), corresponding to a monomeric complex with the anion. The dimer can be completely "melted" by the presence of a large excess of tetrabutylammonium bromide,

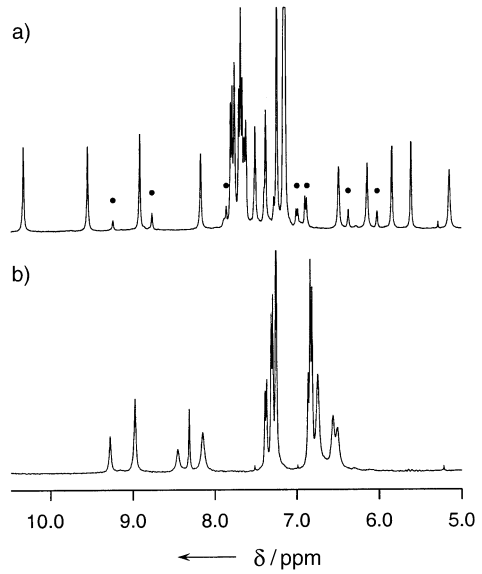

Figure 9. Section of the ^{1}H NMR spectra (400 MHz, [D]chloroform, 298 K) of **2a** in the presence of: a) a 1.5-fold excess of $Et_4N^+ \cdot Br^-$ (signals of monomeric anion complex are indicated with filled circles (●)), b) a 50-fold excess of Bu_4N^+ Br^-.

which cannot be included into the dimeric capsule (Figure 9b).[19]

Computational Studies

Energetic characterization: Several model assemblies of **2a** and **2d** were constructed and submitted to a MD simulation in chloroform boxes: the tetrameric complex and dimeric capsules with the amide residues in both distal and proximal orientations, including either one benzene molecule or one tetraethylammonium cation.

The parent tetraurea dimer $\mathbf{1}_2$, when enclosing suitable neutral guests, is stabilized by a seam of 16 hydrogen bonds, which corresponds to eight hydrogen bonds per monomer. In the capsules of amides **2** this number is reduced to a maximum of seven hydrogen bonds. Molecular dynamics (MD) simulations of $C_6H_6{\cdot}\mathbf{2a}_2$ gave an average of 6.65 hydrogen bonds per subunit both for the distal and for the proximal isomers.

The crystal structure of $\mathbf{2a}_4$ reveals 24 intermolecular hydrogen bonds, of which, on average, 22.8 are present during the MD simulation, corresponding to 5.7 hydrogen bonds per calixarene monomer. Thus, if all other interactions are neglected and the energy gain associated with each hydrogen bond is assumed to be in the range of about 8.3–8.9 kcal mol^{-1}, the monoacetamide capsules should be considerably stabilized over the tetramer. However, the simulations predict the tetramer to be more stable by about ΔE_{inter} = 15 kcal mol^{-1} per subunit (Table 1). The complexation energies $\Delta E_{complex}$, which also include the energy necessary for the reorganization of the molecular structure upon formation of the supramolecular assembly, favor the tetramer by 3.4 kcal mol^{-1}. Since hydrogen bonding alone cannot account for the stabilization of the tetramer, there must be other attractive forces between the monomers in the very compact assembly. The MD trajectories revealed numerous CH···π, NH···π, and π···π interactions, the contributions of which to the stabilization of the tetramer are difficult to quantify. Apparently, the combination of these interactions with hydrogen bonds make the tetramer more advantageous than the dimer.

The interaction of tetraethylammonium tetrafluoroborate with **2a** drives the equilibrium from tetrameric assemblies to dimeric capsules ($\Delta E_{complex} \approx 15$ kcal mol^{-1}). Around 3.6 and 4.3 hydrogen bonds per monomer are predicted in the proximal and distal regioisomers of $\mathbf{2a}_2$, respectively, due to the inclusion of the large Et_4N^+. The weaker hydrogen bonding is compensated for by strong host–guest interactions ($\Delta E_{interact} \approx 65$ kcal mol^{-1} per capsule). The calculated energies of proximal and distal isomers of $Et_4N^+{\cdot}\mathbf{2a}_2{\cdot}BF_4^-$ are the same within their fluctuations and therefore do not explain the higher stability of the distal isomer observed in solution.

For **2d**, the simulations not unexpectedly predict that the two isomeric $Et_4N^+{\cdot}\mathbf{2d}_2{\cdot}BF_4^-$ complexes should be energetically favored over the tetramer by approx. 20 kcal mol^{-1} per subunit. According to the simulations, tetramers $\mathbf{2d}_4$ and the $C_6H_6{\cdot}\mathbf{2d}_2$ dimers should coexist in solution in the absence of the ammonium salt ($\Delta E \approx 1$ kcal mol^{-1}; cf. Table 1).

Geometric characterization: The MD simulations predict that the solution structure of $\mathbf{2a}_4$ should be very similar to the crystal structure (Table 2, Figure 2). Superposition of the crystal structure and the minimized average structure of $\mathbf{2a}_4$ gives a RMS value of 0.39 Å. With a hydrogen bond threshold of 2.7 Å for the D–H···A distance and a minimum of 135° for the D–H···A angle, an average of 22.8 hydrogen bonds is found during the simulation of $\mathbf{2a}_4$ (Table 3). The

Table 2. Geometric parameters of tetrameric assemblies.

	$\mathbf{2a}_4$	$\mathbf{2a}_4$ (X-ray)	$\mathbf{2d}_4$
centers of mass (adjacent, [Å])	8.0	7.9	8.7
centers of mass (diagonal, [Å])	10.9	10.9	11.9
amide carbonyl carbon distance (adjacent, [Å])	4.2	4.1	5.1
amide carbonyl carbon distance (diagonal, [Å])	5.9	5.7	6.7
methylene planes (adjacent, [°])	55	56	72
methylene planes (diagonal, [°])	81	83	66
angle between aryl planes **A**–**II** ([°])	25	25	18
angle between aryl planes **I**–**III** ([°])	110	108	114
RMS[a] ([Å])	0.43	0.0	1.55

[a] Hydrogens, tolyl, and ether group atoms are neglected.

Table 1. Energetic analysis of tetrameric and dimeric assemblies. Fluctuations are given in parenthesis.

	$\Delta E_{complex}$[a] [kcal mol^{-1}]	ΔE_{int}[b] [kcal mol^{-1}]	$\Delta E_{int\ total}$[c] [kcal mol^{-1}]	Average number of hydrogen bonds
$\mathbf{2a}_4$	−64.1 (4.6)	−69.7 (1.5)	−69.7 (1.5)	22.8
$\mathbf{2d}_4$	−53.9 (4.2)	−62.0 (1.7)	−62.0 (1.7)	22.2
$C_6H_6{\cdot}\mathbf{2a}_2$ distal isomer	−60.7 (6.1)	−54.3 (1.8)	−65.1 (1.9)	13.3
$C_6H_6{\cdot}\mathbf{2a}_2$ proximal isomer	−60.3 (6.3)	−54.0 (1.7)	−64.9 (1.8)	13.3
$Et_4N^+{\cdot}\mathbf{2a}_2{\cdot}BF_4^-$ distal isomer	−79.4 (6.6)	−37.0 (1.7)	−121.2 (2.4)	7.4
$Et_4N^+{\cdot}\mathbf{2a}_2{\cdot}BF_4^-$ proximal isomer	−80.0 (6.9)	−35.8 (1.8)	−125.3 (2.2)	7.2
$C_6H_6{\cdot}\mathbf{2d}_2$ distal isomer	−52.6 (6.6)	−51.2 (1.6)	−62.2 (1.6)	12.7
$C_6H_6{\cdot}\mathbf{2d}_2$ proximal isomer	−53.2 (6.2)	−50.9 (1.8)	−61.9 (1.8)	12.8
$Et_4N^+{\cdot}\mathbf{2d}_2{\cdot}BF_4^-$ distal isomer	−73.0 (6.5)	−40.4 (1.8)	−122.8 (2.3)	8.8
$Et_4N^+{\cdot}\mathbf{2d}_2{\cdot}BF_4^-$ proximal isomer	−77.3 (6.1)	−38.5 (1.8)	−125.3 (2.3)	7.4

[a] $\Delta E_{complex}$ = complexation energy per subunit = $(E_{total} - E_{guest} - nE_{subunit})/n$; n = number of calixarene subunits, E_{guest} = 0 in the case of the tetramers; [b] $\Delta E_{interact}$ = interaction energy per subunit = $1/n\Delta E_{interaction}$ (calixarene···calixarene); [c] $\Delta E_{interact\ total}$ = interaction energy per subunit, also including host–guest interactions (and anion interaction where applicable).

Table 3. Hydrogen bond analysis for the tetrameric complexes (for atom numbering see Figure 3). Values are averages over all symmetry-equivalent hydrogen bonds. Values are indicated by an asterisk if the hydrogen bond criterion is not fulfilled.

Hydrogen bond	A···D distance [Å]			A···H–D distance [Å]			A···H–D angle [°]			Occurrence[%]	
(A···H–D)	$\mathbf{2a}_4$	X-ray	$\mathbf{2d}_4$	$\mathbf{2a}_4$	X-ray	$\mathbf{2d}_4$	$\mathbf{2a}_4$	X-ray	$\mathbf{2d}_4$	$\mathbf{2a}_4$	$\mathbf{2d}_4$
O105–N304	2.92	2.95	3.03	2.05	2.23	2.12	145	140	151	77	92
O105–N305	3.28	3.66	2.93	2.48	3.16*	2.00	137	118*	155	51	94
O105–N301	3.08	2.95	4.96	2.20	2.14	4.30*	148	154	131*	79	0
O307–N206	3.22	3.29	3.05	2.39	2.56	2.21	141	138	141	67	72
O307–N207	2.87	2.84	2.87	1.92	1.98	1.94	159	165	154	97	95
O208–N306	3.02	3.12	3.01	2.12	2.38	2.09	150	142	152	85	91
O208–N307	3.12	2.98	3.04	2.22	2.21	2.11	150	146	154	86	95
N301–N304	3.58	3.51	4.02	2.80*	2.83*	3.13*	136	135*	151	26	9

hydrogen bonding pattern is nearly unaltered throughout the simulations, but remarkably, four NH hydrogens toggle between a N–H···π interaction as found in the X-ray structure and a hydrogen bond to the acetamide carbonyls, with a relative occupancy of about 50%. In general, the geometry of the hydrogen bonds in the simulated structure correlates well with the crystal structure (Table 3). On average, the D–H···A distances and the D–H···A angles differ by only 0.16 Å and 8°, respectively.

For $\mathbf{2d}_4$ the picture clearly changes. The shortest distance between the amide carbon atoms increases from 4.2 Å in the optimized structure of $\mathbf{2a}_4$ to 5.1 Å in $\mathbf{2d}_4$, due to the additional methylene group, in the core of the assembly. This congestion impacts on all other structural parameters (see Table 2) including the hydrogen bonding motif. Although the cyclic hydrogen-bonded array of the amide residues disappears, the average number of hydrogen bonds is only slightly decreased (22.2 in $\mathbf{2d}_4$ versus 22.8 in $\mathbf{2a}_4$), since three-centered hydrogen bonds to the propionamide carbonyl occur instead. Nearly all other hydrogen bonds are stronger and occur more frequently in $\mathbf{2d}_4$ (Table 3). Thus, as judged from the hydrogen bonding pattern observed in the simulations of $\mathbf{2d}_4$ and from the energetic analysis (vide supra), it is difficult to explain why the tetrameric assembly has not been observed experimentally. It is, however, interesting to note that all the polar groups in $\mathbf{2a}_4$ are buried below the non-polar surface (Figure 10, left) whereas the congestion in the core of $\mathbf{2d}_4$ leads to the exposure of polar groups to the assembly surface (Figure 10, right). This makes the whole complex susceptible to aggregation in non-polar solvents, as observed in [D]chloroform.

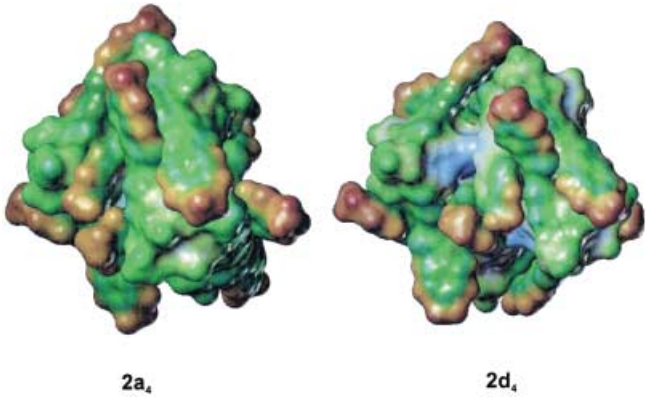

Figure 10. Lipophilic potentials of the optimized tetrameric assemblies. Blue and brown zones mark hydrophilic and lipophilic regions, respectively.

Conclusion

Calix[4]arenes substituted at the wide rim by three arylurea functions and one amide group are readily available. They present a striking example of how apparently small changes in the size and the hydrogen-bonding ability of functional groups in single molecules may cause drastic changes in stoichiometry, size, and properties of the emergent supramolecular assemblies and of how these assemblies can be triggered by suitable guests and by the solvent. Triurea monoacetamides, like the analogous tetraureas, exist as monomers in polar solvents. In apolar solvents they form stable tetrameric assemblies held together by a novel pattern or motif of hydrogen bonding, also found in the crystalline state. The high stabilities of these tetramers in solution are due to cooperation of multiple NH···O=C hydrogen bonds in combination with weaker NH···π, CH···π, and π···π attractions. Even a slight increase in the size of the amide group leads to ill-defined assemblies, while the addition of tetraethylammonium cations, known as excellent guests for tetraurea capsules, induces the formation of dimeric capsules irrespective of the size of the amide group.

Experimental Section

Reagents and methods: The 1D ^{1}H and 2D COSY, NOESY, ROESY, TOCSY and ^{1}H–^{15}N HMBC NMR spectra were recorded with Bruker Avance DRX 500 (500 MHz) and DRX 400 (400 MHz), Bruker DPX 250 (250 MHz), and Bruker 200 (200 MHz) spectrometers with the solvent signals as internal reference. FD mass spectra were recorded with a Finnigan MAT 90 instrument (5 kV/10 mA min^{-1}). Melting points were determined with a MEL TEMP 2 capillary melting point apparatus and are uncorrected. Compound **4** was prepared by a known procedure.[13] Guests were purchased from Aldrich and were used without further purification.

General procedure for the synthesis of 5a–c: The isocyanate (2.5 mmol) was added in one portion under an argon atmosphere to a stirred solution of the triamine **4** (0.5 mmol) in dry THF (5 mL) and the reaction mixture was stirred at room temperature overnight. Hexane was added, and the precipitate was filtered off and dried in vacuo to give a white solid, which was further purified either by recrystallization from $CHCl_3$/methanol or by column chromatography (ethyl acetate).

Tri-tolylurea mono-Boc-calix[4]arene 5a: Yield 79%; m.p.: 115–116°C; ^{1}H NMR (400 MHz, [D$_6$]DMSO): δ = 8.98 (s, 1H; NH), 8.31 (s, 2H; NH), 8.10 (s, 2H; NH), 7.98 (s, 2H; NH), 7.28 (d, ^2J = 8.5 Hz, 2H; ArH), 7.14 (d, ^2J = 8.24 Hz, 4H; ArH), 7.04–6.97 (m, 10H; ArH), 6.56 (s, 2H; ArH), 6.51 (s, 2H; ArH), 4.30 (d, ^2J = 12.6 Hz, 2H; ArCH$_2$Ar), 4.29 (d, ^2J = 12.3 Hz, 2H; ArCH$_2$Ar), 3.87 (br m, 4H; ArOCH$_2$), 3.68 (t, J = 6.4 Hz, 4H; ArOCH$_2$), 3.08 (d, ^2J = 12.9 Hz, 2H; ArCH$_2$Ar), 3.02 (d, ^2J = 12.5 Hz, 2H; ArCH$_2$Ar), 2.17 (s, 3H; ArCH$_3$), 2.19 (s, 6H; ArCH$_3$), 1.96–1.81 (m, 8H; CH$_2$), 1.52–1.21 (m, 25H; CH$_2$ and C(CH$_3$)$_3$), 0.93–0.90 ppm (m, 12H; CH$_3$); FD-MS: *m/z* (%): 1264.2 (100) $[M]^+$.

Tri-methoxyphenylurea mono-Boc-calix[4]arene 5b: Yield 79%; m.p.: 150–151°C; ^{1}H NMR (200 MHz, [D$_6$]DMSO): δ = 8.83 (s, 1H; NH), 8.15 (s, 4H; NH), 8.08 (s, 2H; NH), 7.29–7.21 (m, 6H; ArH), 6.82–6.74 (m, 12H; ArH), 5.97 (s, 2H; ArH), 4.32 (d, ^2J = 13.2 Hz, 2H; ArCH$_2$Ar), 4.23 (d, ^2J = 12.8 Hz, 2H; ArCH$_2$Ar), 3.80–374 (m, 8H; ArOCH$_2$), 3.68 (s, 6H; ArOCH$_3$), 3.67 (s, 3H; ArOCH$_3$), 3.07 (d, ^2J = 13.5 Hz, 2H; ArCH$_2$Ar), 2.93 (d, ^2J = 12.8 Hz, 2H; ArCH$_2$Ar), 1.88 (br s, 8H; CH$_2$), 1.54 (s, 9H; C(CH$_3$)$_3$), 1.36 (br s, 16H; CH$_2$), 0.95–0.88 ppm (m, 12H; CH$_3$); FD-MS: *m/z* (%): 1312.3 (100) $[M]^+$.

Tri-hexylurea mono-Boc-calix[4]arene 5c: Yield 80%; m.p.: 98–100°C; ^{1}H NMR (400 MHz, [D$_6$]DMSO): δ = 8.84 (s, 1H; NH), 7.98 (s, 1H; NH), 7.75 (s, 2H; NH), 6.90 (s, 2H; ArH), 6.80 (s, 2H; ArH), 6.49 (s, 2H; ArH), 6.46 (s, 2H; ArH), 5.81 (t, ^3J = 5.8 Hz, 1H; NH), 5.66 (t, ^3J = 5.5 Hz 2H; NH), 4.24 (d, ^2J = 12.2 Hz, 4H; ArCH$_2$Ar), 3.82 (br s, 4H; ArOCH$_2$), 3.65 (t, ^3J = 6.6 Hz, 4H; ArOCH$_2$), 3.01–2.89 (m, 10H; NCH$_2$ and ArCH$_2$Ar), 1.88–1.78 (m, 8H; CH$_2$), 1.39 (s, 9H; C(CH$_3$)$_3$), 1.37–1.19 (m, 28H; CH$_2$), 0.88 (t, ^3J = 6.6 Hz, 12H; CH$_3$), 0.81 ppm (m, 9H; CH$_3$); FD-MS: *m/z* (%): 1245.5 (100) $[M]^+$.

Triurea monoamine calix[4]arenes 6a–c: TFA (20 mL) was added in one portion to a solution of **5a–c** (0.3 mmol) in CH$_2$Cl$_2$ (20 mL). The reaction mixture was stirred at room temperature for 2 h and was then diluted with toluene (50 mL). The solvent was evaporated to dryness in vacuo to give the crude product as a yellowish powder. Precipitation from CHCl$_3$/hexane gave the desired amines **6a–c** as their triflate salts.

Tri-tolylurea monoamine calix[4]arene 6a: Yield 98%; m.p. > 300°C; ^{1}H NMR (400 MHz, [D$_6$]DMSO): δ = 9.27 (br s, 2H; ArNH$_2$), 8.54 (s, 2H; NH), 8.47 (s, 2H; NH), 8.34 (s, 1H; NH), 8.18 (s, 1H; NH), 7.28 (d, ^3J = 8.2 Hz, 4H; ArH), 7.22 (d, ^3J = 8.2 Hz, 2H; ArH), 7.14 (s, 2H; ArH), 7.04–7.00 (m, 6H; ArH), 6.94 (s, 2H; ArH), 6.63 (s, 2H; ArH), 6.53 (s, 2H; ArH), 4.35 (d, ^2J = 13.5 Hz, 2H; ArCH$_2$Ar), 4.31 (d, ^2J = 13.5 Hz, 2H; ArCH$_2$Ar), 3.94–3.84 (m, 4H; ArOCH$_2$), 3.75 (t, ^3J = 6.7 Hz, 2H; ArOCH$_2$), 3.70 (t, ^3J = 6.7 Hz, 2H; ArOCH$_2$), 3.19 (d, ^2J = 12.9 Hz, 2H; ArCH$_2$Ar), 3.11 (d, ^2J = 13.2 Hz, 2H; ArCH$_2$Ar), 2.21 (s, 6H; ArCH$_3$), 2.19 (s, 3H; ArCH$_3$), 1.95–1.85 (m, 8H; CH$_2$), 1.43–1.30 (m, 16H; CH$_2$), 0.92 ppm (t, ^3J = 6.7 Hz, 12H; CH$_3$); FD-MS: *m/z* (%): 1161.5 (100) $[M]^+$.

Tri-methoxyphenylurea monoamine calix[4]arene 6b: Yield 88%; m.p. > 300°C; ^{1}H NMR (200 MHz, [D$_6$]DMSO): δ = 9.31 (br s, 2H; ArNH$_2$), 8.20 (s, 4H; NH), 8.10 (s, 2H; NH), 7.27 (d, ^3J = 8.7 Hz, 2H; ArH), 7.22 (d, ^3J = 8.8 Hz, 4H; ArH), 6.82–6.74 (m, 12H; ArH), 5.97 (s, 2H; ArH), 4.31 (d, ^2J = 12.5 Hz, 2H; ArCH$_2$Ar), 4.25 (d, ^2J = 12.8 Hz, 2H; ArCH$_2$Ar), 3.80–374 (m, 8H; ArOCH$_2$), 3.68 (s, 6H; ArOCH$_3$), 3.67 (s, 3H; ArOCH$_3$), 3.07 (d, ^2J = 13.5 Hz, 2H; ArCH$_2$Ar), 2.93 (d, ^2J = 12.8 Hz, 2H; ArCH$_2$Ar), 1.88 (br s, 8H; CH$_2$), 1.36 (br s, 16H; CH$_2$), 0.91 ppm (t, ^3J = 6.5 Hz, 12H; CH$_3$); FD-MS: *m/z* (%): 1209.4 (100) $[M]^+$.

Tri-hexylurea monoamine calix[4]arene 6c: Yield 99%, mp > 300°C; ^{1}H NMR (400 MHz, [D$_6$]DMSO): δ = 9.26 (br s, 2H; NH$_2$), 8.38 (s, 2H; NH), 8.06 (s, 1H; NH), 7.33 (s, 2H; ArH), 7.14 (s, 2H; ArH), 6.69 (s, 2H; ArH), 6.62 (s, 2H; ArH), 6.25 (t, ^3J = 5.1 Hz, 2H; NH), 6.17 (t, ^3J = 5.0 Hz, 1H; NH), 4.55 (d, ^2J = 12.8 Hz, 2H; ArCH$_2$Ar), 4.50 (d, ^2J = 12.5 Hz, 2H; ArCH$_2$Ar), 4.18–4.06 (m, 4H; ArOCH$_2$), 3.95 (t, ^3J = 6.2 Hz, 2H; ArOCH$_2$), 3.87 (t, ^3J = 6.0 Hz, 2H; ArOCH$_2$), 3.36 (d, ^2J = 12.5 Hz, 2H; ArCH$_2$Ar), 3.29–3.17 (m, 8H; ArCH$_2$Ar and NCH$_2$), 2.19–2.05 (m, 6H; CH$_2$), 2.00–1.97 (m, 2H; CH$_2$), 1.69–1.58 (m, 12H; CH$_2$), 1.50 (br s, 16H; CH$_2$), 1.15 (t, ^3J = 6.3 Hz, 12H; CH$_3$), 1.12–1.07 ppm (m, 9H; CH$_3$); FD-MS: *m/z* (%): 1143.8 (100) $[M]^+$.

Tri-tolylurea monoacetamide calix[4]arene 2a: NEt$_3$ (0.5 mL) was added in one portion to a solution of the monoamine **6a** (200 mg, 0.17 mmol) in Ac$_2$O (20 mL), and the reaction mixture was stirred at room temperature overnight. The precipitate formed was filtered off, washed with water and methanol, and dried in vacuo. Compound **2a**: yield 78%; white solid. The spectra were as described in reference [13].

Tri-methoxyphenylurea monoacetamide calix[4]arene 2b: This compound was prepared in the same way as **2a**, from monoamine **6b**, Ac$_2$O, and NEt$_3$. Compound **2b**: yield 90%; yellowish solid; m.p.: 187–189°C; ^{1}H NMR (200 MHz, [D$_6$]DMSO): δ = 9.46 (s, 1H; NH), 8.19 (s, 1H; NH), 8.15 (s, 2H; NH), 8.10 (s, 2H; NH), 8.06 (s, 1H; NH), 7.29–7.21 (m, 6H; ArH), 6.94 (s, 2H; ArH), 6.82–6.76 (m, 12H; ArH), 4.31 (d, ^2J = 12.5 Hz, 4H; ArCH$_2$Ar), 3.79 (t, ^3J = 7.1 Hz, 8H; ArOCH$_2$), 3.68 (s, 9H; ArOCH$_3$), 3.07 (d, ^2J = 12.8 Hz, 4H; ArCH$_2$Ar), 2.07 (s, 3H; COCH$_3$), 1.98–1.77 (m, 8H; CH$_2$), 1.48–1.28 (m, 16H; CH$_2$), 0.92 ppm (t, ^3J = 6.5 Hz, 12H; CH$_3$); FD-MS: *m/z* (%): 1255.4 (100) $[M]^+$.

Tri-hexylurea monoacetamide calix[4]arene 2c: This compound was prepared in the same way as **2a**, from monoamine **6c**, Ac$_2$O, and NEt$_3$. Compound **2c**: yield 75%; white powder; m.p.: 157–159°C; ^{1}H NMR (400 MHz, [D$_6$]DMSO): δ = 9.51 (s, 1H; NH), 8.36 (s, 2H; NH), 8.10 (s, 1H; NH), 7.32 (s, 2H; ArH), 7.15 (s, 2H; ArH), 6.71 (s, 2H; ArH), 6.60 (s, 2H; ArH), 6.24 (t, ^3J = 5.5 Hz, 2H; NH), 6.17 (t, ^3J = 5.2 Hz, 1H; NH), 4.53 (d, ^2J = 13.5 Hz, 2H; ArCH$_2$Ar), 4.47 (d, ^2J = 12.8 Hz, 2H; ArCH$_2$Ar), 4.22–4.10 (m, 4H; ArOCH$_2$), 3.90 (t, ^3J = 5.3 Hz, 2H; ArOCH$_2$), 3.87 (t, ^3J = 6.2 Hz, 2H; ArOCH$_2$), 3.37 (d, ^2J = 13.5 Hz, 2H; ArCH$_2$Ar), 3.27–3.14 (m, 8H; ArCH$_2$Ar and NCH$_2$), 2.17 (br s, 6H; CH$_2$), 1.99–1.95 (m, 2H; CH$_2$), 1.69–1.58 (m, 12H; CH$_2$), 1.50 (br s, 16H; CH$_2$), 1.17 (t, ^3J = 6.2 Hz, 12H; CH$_3$), 1.08 ppm (br s, 9H; CH$_3$); FD-MS: *m/z* (%): 1187.6 (100) $[M]^+$.

Tri-tolylurea monopropionamide calix[4]arene 2d: Propionyl chloride (0.5–1 mL) was added to a vigorously stirred suspension of monoamine **2a** (200 mg, 0.17 mmol) in EtOAc (20 mL) and Na$_2$CO$_3$ (1 N, 40 mL). The mixture was intensively stirred at room temperature for 2 h (reaction monitored by TLC). The organic layer was separated, and washed with Na$_2$CO$_3$ (1 N, 50 mL) and water (2 × 50 mL). The solvent was removed in vacuo, and the residue was dissolved in CHCl$_3$ and reprecipitated with hexane to give a white solid. Compound **2e**: yield 85%; m.p.: 185–187°C; ^{1}H NMR (400 MHz, [D$_6$]DMSO): δ = 9.30 (s, 1H; NH), 8.18 (s, 1H; NH), 8.14 (s, 2H; NH), 8.05 (s, 1H; NH), 8.02 (s, 2H; NH), 7.14 (d, ^3J = 8.2 Hz, 2H; ArH), 7.09 (d, ^3J = 8.4 Hz, 4H; ArH), 6.92–6.89 (m, 6H; ArH), 6.71 (s, 4H; ArH), 6.64 (s, 2H; ArH), 6.59 (s, 2H; ArH), 4.20 (d, ^2J = 12.5 Hz, 4H; ArCH$_2$Ar), 3.72–3.66 (m, 8H; ArOCH$_2$), 2.98 (d, ^2J = 12.5 Hz, 2H; ArCH$_2$Ar), 2.95 (d, ^2J = 12.5 Hz, 2H; ArCH$_2$Ar), 2.09 (s, 9H; ArCH$_3$), 1.78 (br s, 8H; CH$_2$), 1.28–1.26 (m, 16H; CH$_2$), 1.02 (t, ^3J = 6.2 Hz, 3H; CH$_3$), 0.88–0.81 ppm (m, 15H; CH$_3$ and CH$_2$); FD-MS: *m/z* (%): 1221.9 (100) $[M]^+$.

Tri-tolylurea monovaleramide calix[4]arene 2e: This compound was prepared in the same way as **2d**, from monoamine **6a** (200 mg, 0.17 mmol) and valeroyl chloride (0.5–1 mL). Yield 80%; white powder: m.p.: 196–198°C; ^{1}H NMR (400 MHz, [D$_6$]DMSO): δ = 9.42 (s, 1H; NH), 8.26 (s, 1H; NH), 8.19 (s, 2H; NH), 8.14 (s, 1H; NH), 8.10 (s, 2H; NH), 7.26 (d, ^3J = 8.2 Hz, 2H; ArH), 7.21 (d, ^3J = 8.2 Hz, 4H; ArH), 7.04–7.01 (m, 6H; ArH), 6.83 (s, 4H; ArH), 6.76 (s, 2H; ArH), 6.71 (s, 2H; ArH), 4.32 (d, ^2J = 12.5 Hz, 4H; ArCH$_2$Ar), 3.84–3.77 (m, 8H), 3.10 (d, ^2J = 12.5 Hz, 2H; ArCH$_2$Ar), 3.07 (d, ^2J = 12.5 Hz, 2H; ArCH$_2$Ar), 2.21 (s, 9H; ArCH$_3$), 2.19–2.16 (m, 2H; COCH$_2$), 1.89 (m, 8H; CH$_2$), 1.51–1.43 (m, 2H; CH$_2$), 1,39–1.38 (m, 16H; CH$_2$), 1.25–1.19 (m, 2H; CH$_2$), 0.94–0.91 (m, 12H; CH$_3$), 0.82 ppm (t, ^3J = 6.2 Hz, 3H; CH$_3$); FD-MS: *m/z* (%): 1250.0 (100) $[M]^+$.

Tri-tolylurea mono-p-methylbenzamide calix[4]arene 2f: This compound was prepared in the same way as **2d**, from monoamine **6a** and *p*-methylbenzoyl chloride. Yield 86%; Brown solid: m.p.: 260–261°C; ^{1}H NMR (400 MHz, [D$_6$]DMSO): δ = 9.86 (s, 1H; NH), 8.23 (s, 1H; NH), 8.20 (s, 1H; NH), 8.16 (s, 2H; NH), 8.06 (s, 2H; NH), 7.78 (d, ^3J = 7.9 Hz, 2H; ArH), 7.29 (s, 2H; ArH), 7.23–7.15 (m, 8H; ArH), 7.03–6.97 (m, 6H; ArH), 6.89 (s, 2H; ArH), 6.71 (d, ^3J = 2.0 Hz, 2H; ArH), 6.66 (d, ^3J = 2.1 Hz, 2H; ArH), 4.34 (d, ^2J = 13.2 Hz, 2H; ArCH$_2$Ar), 4.30 (d, ^2J = 13.5 Hz, 2H; ArCH$_2$Ar), 3.89–3.83 (m, 4H; ArOCH$_2$), 3.76 (t, ^3J = 7.0 Hz, 4H; ArOCH$_2$), 3.12–3.08 (m, 4H; ArCH$_2$Ar), 2.30 (s, 3H; ArCH$_3$), 2.20 (s, 3H; ArCH$_3$), 2.18 (s, 6H; ArCH$_3$), 1.96–1.84 (m, 8H; CH$_2$), 1.39–1.37 (m, 16H; CH$_2$), 0.92 ppm (t, ^3J = 6.2 Hz, 12H; CH$_3$); FD-MS: *m/z* (%): 1283.2 (100) $[M]^+$.

Single-crystal X-ray analysis: Measurements were made at 173.0(2) K with an Enraf Nonius Kappa CCD diffractometer, $Mo_{K\alpha}$ radiation, λ = 0.71073 Å. The data were processed with Denzo-SMN v 0.93.0.[20] The structures were solved in the $P1$ space group by use of shake and bake methods as implemented in the XM program.[21] The transformation to the $P\bar{1}$ space group was performed by use of the XP program,[22] refinements on F^2 by SHELXL-97.[23] These procedures were run under Wingx program[24] Four calixarene molecules constituting the tetramer and solvent molecules were refined in separate blocks. The hydrogen atoms were normally calculated to their idealized positions with isotropic temperature factors and refined as riding atoms. Disordered solvent molecules and parts of pendant alkyl chains were treated isotropically in some cases. No attempts were made to localize hydrogen atoms in the disordered parts of the structure. Geometrical restraints were imposed on disordered parts of the structures to keep the interatomic distances in reasonable ranges. The intense peaks which could not be recombined to acetonitrile or dichloromethane molecules were treated as oxygen atoms (possibly water).

CCDC 149022–CCDC-149029 contain the supplementary crystallographic data for this paper. These data can be obtained free of charge via www.ccdc.can.ac.uk/conts/retrieving.html (or from the Cambridge Crystallographic Center, 12 Union Road, Cambridge CB2 1EZ, UK; Fax: (+44) 1223-336033; or deposit@ccdc.cam.ac.uk).

Compound 2a$_4$: triclinic $P\bar{1}$, a = 21.4219(3), b = 25.7044(3), c = 29.9918(3) Å, α = 87.305(2), β = 86.041(2), γ = 79.250(2)°, Z = 2, V = 16176.2(4) Å^3, ρ = 1.11 g cm^{-3}, μ = 0.169 cm^{-1}, $2\theta_{max}$ = 50.1°, $R1$ = 0.155, $wR2$ = 0.43 (for 30545 reflections $I > 2\sigma(I)$), $R1$ = 0.2376, $wR2$ = 0.5029 (for 56601 independent reflections), 3621 parameters, S = 1.098, $\Delta\rho$ (max/min) = 1.20/0.92 e Å^{-3}. The strongest residual peaks are located near disordered solvent molecules.

Dynamic NOE studies: Under certain conditions NOE is proportional to mixing time. The cross-relaxation constant (σ_{IS}) is the slope of this dependence. It is defined by the following formula

$$\sigma_{IS} = \left(\frac{\mu_0}{4\pi}\right)^2 \frac{\hbar^2\gamma^4}{10}\left[\frac{6\tau_c}{1+4\omega^2\tau_c^2}-\tau_c\right] r_{IS}^{-6} \quad (1)$$

where τ_c = correlation rotational time, r_{IS} is the distance between protons, T is absolute temperature, ω and γ are the Larmour frequency and the gyromagnetic ratio for ^{1}H, μ_0 = magnetic constant of a vacuum, and $\hbar$ = Plank's constant divided by 2π (see reference [15,16]). For the simplest case of a spherical molecule (aggregate), correlation time is the time necessary for a molecule (aggregate) to tumble through an angle of one radian. In accordance with Stokes' law $\tau_c = 4\pi r^3\eta/3kT$, where η is the viscosity of the solvent, k is Boltzmann's constant, and r is the radius of the molecule or aggregate.

VPO studies: A KNAUER K-7000 vapor pressure osmometer was used to carry out VPO measurements on **2a** in benzene solution at 303 K. The tetradecyl ether of tetra-*tert*-butylcalix[4]arene and the tetratolyl urea of the calix[4]arene with four decyl groups at the narrow rim (**1**: R = *p*-tolyl, Y = $C_{10}H_{21}$)[25] were used for calibration of the instrument.

Methods of calculations: All calculations were performed by employment of version 6 of the AMBER[26] program suite. Initial geometries were obtained from the crystal structure of a dimeric calixarene capsule (CSD-refcode TIDWEI) by modification by SYBYL[27] and from the raw coordinates (before final refinement) of the X-ray structure of the tetrameric assembly. To save calculation time methyl or ethyl groups were used instead of the original pentyl moieties. The starting structure of the tetrameric assembly was generated from these data by turning the pentyl side chains R into ethyl residues. RESP charges[28] were assigned, and the whole assembly was solvated in a chloroform box (14 Å solvent layer thickness on each side). Prior to each simulation, 5000 minimization steps followed by 30 ps belly dynamics and 100 ps equilibration at 300 K and 1 bar were carried out. During 9 ns of simulation time with a time step of 1 fs, the ensembles were kept at 1 bar and 300 K by use of the Berendsen algorithm,[29] an experimental compressibility of 100×10^{-6} bar^{-1}, 1.0 ps pressure coupling time, and 0.5 ps temperature coupling time. Bonds containing hydrogen were constrained to the equilibrium bond length by use of the SHAKE algorithm. Snapshots were recorded every 2000 steps. The C_{Ar}–N rotational barrier was set to 2.3 kcal mol^{-1} to reproduce the value obtained by 6-31G**/MP2 calculations.

Analysis of hydrogen bonds was conducted by measurement of distances and angles between potential donor and acceptor sites for each snapshot of the trajectory followed by statistical summarization.

Acknowledgement

This work was financially supported by the Finnish Academy and by the Deutsche Forschungsgemeinschaft (grant Th 520/5–1, Bo 523/14–2). We warmly thank Professor Erich F. Paulus (University of Frankfurt/Main, Germany) for valuable crystallographic advice. Mr. Rejo Kauppinen is acknowledged for technical help with NMR measurements. We thank Mr. Liam Palmer (TSRI) for critically reading the manuscript and valuable suggestions.

[1] a) K. D. Shimizu, J. Rebek, Jr., *Proc. Natl. Acad. Sci. USA* **1995**, *92*, 12403–12407; b) O. Mogck, V. Böhmer, W. Vogt, *Tetrahedron* **1996**, *52*, 8489–8496; c) B. C. Hamman, K. D. Shimizu, J. Rebek, Jr., *Angew. Chem.* **1996**, *108*, 1425–1427; *Angew. Chem. Int. Ed. Engl.* **1996**, *35*, 1326–1329.

[2] O. Mogck, E. F. Paulus, V. Böhmer, I. Thondorf, W. Vogt, *Chem. Commun.* **1996**, 2533–2534.

[3] I. Thondorf, F. Broda, K. Rissanen, M. O. Vysotsky, V. Böhmer, *J. Chem. Soc. Perkin Trans. 2* **2002**, 1796–1800.

[4] a) R. K. Castellano, D. M. Rudkevich, J. Rebek, Jr., *Proc. Natl. Acad. Sci. USA*. **1997**, *94*, 7132–7137; b) R. K. Castellano, C. Nuckolls, S. H. Eichhorn, M. R. Wood, A. J. Lovinger, J. Rebek, Jr., *Angew. Chem.* **1999**, *111*, 2764–2768; *Angew. Chem. Int. Ed.* **1999**, *38*, 2603–2606.

[5] a) O. Mogck, M. Pons, V. Böhmer, W. Vogt, *J. Am. Chem. Soc.* **1997**, *119*, 5706–5712; b) R. K. Castellano, C. Nuckolls, J. Rebek, Jr., *J. Am. Chem. Soc.* **1999**, *121* , 11156–11163; c) A. Pop, M. O. Vysotsky, M. Saadioui, V. Böhmer, *Chem. Commun.* **2003**, 1124–1125.

[6] M. S. Brody, C. A. Schalley, D. M. Rudkevich, J. Rebek, Jr., *Angew. Chem.* **1999**, *111*, 1738–1742; *Angew. Chem. Int. Ed.* **1999**, *38*, 1640–1644.

[7] M. O. Vysotsky, I. Thondorf, V. Böhmer, *Angew. Chem.* **2000**, *112*, 1309–1312; *Angew. Chem. Int. Ed.* **2000**, *39*, 1264–1267.

[8] M. O. Vysotsky, I. Thondorf, V. Böhmer, *Chem. Commun.* **2001**, 1890–1891.

[9] A. M. Rincon, P. Prados, J. de Mendoza, *J. Am. Chem. Soc.* **2001**, *123*, 3493–3498; for an example derived from a trisubstituted calix[6]arene see: J. J. González, R. Ferdani, E. Albertini, J. M. Blasco, A. Arduini, A. Pochini, P. Prados, J. de Mendoza, *Chem. Eur. J.* **2000**, *6*, 73–80.

[10] R. E. Brewster, S. B. Shuker, *J. Am. Chem. Soc.* **2002**, *124*, 7902–7903.

[11] a) R. Zadmard, T. Schrader, T. Grawe, A. Kraft, *Org. Lett.* **2002**, *4*, 1687–1690; b) F. Corbellini, R. Fiammengo, P. Timmerman, M. Crego-Calama, K. Versluis, A. J. R. Heck, I. Luyten, D. N. Reinhoudt, *J. Am. Chem. Soc.* **2002**, *124*, 6569–6575.

[12] R. K. Castellano, B. H. Kim, J. Rebek, Jr., *J. Am. Chem. Soc.* **1997**, *119*, 12671–12672.

[13] M. Saadioui, A. Shivanyuk, V. Böhmer, W. Vogt, *J. Org. Chem.* **1999**, *64*, 3774–3777.

[14] M. Conner, V. Janout, S. L. Regen, *J. Am. Chem. Soc.* **1991**, *113*, 9670–9671.

[15] D. Neuhaus, N. Williamson, *The Nuclear Overhauser Effect In Structural and Conformational Analysis*, VCH, New York, **1989**.

[16] This technique was applied for the size evaluation of hexameric calix[4]arene rosettes: R. H. Vreekamp, J. P. M. van Duynhoven, M. Hubert, W. Verboom, D. N. Reinhoudt, *Angew. Chem.* **1996**, *108*, 1306–1309; *Angew. Chem. Int. Ed. Engl.* **1996**, *35*, 1215–1218.

[17] Similar processes for dimeric capsules of tetraurea calix[4]arene derivatives: M. O. Vysotsky, A. Pop, F. Broda, I. Thondorf, V. Böhmer, *Chem. Eur. J.* **2001**, *7*, 4403–4410.

[18] J. Scheerder, J. P. M. van Duynhoven, J. F. J. Engbersen, D. N. Reinhoudt *Angew. Chem.* **1996**, *108*, 1172–1174; *Angew. Chem. Int. Ed. Engl.* **1996**, *35*, 1090–1093.
[19] Similar behavior was also observed for other molecular capsules: a) A. Shivanyuk, J. Rebek, Jr., *Proc. Natl. Acad. Sci. USA* **2001**, *98*, 7662–7665; b) A. Shivanyuk, J. Rebek, Jr., *Chem. Commun.* **2001**, 2374–2375.
[20] Z. Otwinowski, W. Minor *"Processing of X-ray Diffraction Data Collected in Oscillation Mode"* Methods in Enzymology, Vol. 276: Macromolecular Crystallography, part A, (Eds.: C. W. Carter, Jr., R. M. Sweet), Academic Press, **1997**, 307–326.
[21] Macromolecular Direct Methods, XM, Ver. 6.09, Bruker-AXS, **2000**.
[22] XP Interactive Molecular Graphics. Version 5.1. 1998. Bruker AXS.
[23] G. M. Sheldrick, SHELXL-97, Program for the Refinement of Crystal Structures. Universität Göttingen, Germany, **1997**.
[24] L. J. Farrugia, *J. Appl. Crystallogr.* **1999**, *32*, 837–838.
[25] M. O. Vysotsky, V. Böhmer, *Org. Lett.* **2000**, *2*, 3571–3574.
[26] D. A. Case, D. A. Pearlman, J. W. Caldwell, T. E. Cheatham III, W. S. Ross, C. L. Simmerling, T. A. Darden, K. M. Merz, R. V. Stanton, A. L. Cheng, J. J. Vincent, M. Crowley, V. Tsui, R. J. Radmer, Y. Duan, J. Pitera, I. Massova, G. L. Seibel, U. C. Singh, P. K. Weiner, P. A. Kollman, **1999**, AMBER6, University of California, San Francisco.
[27] SYBYL 6.8 Tripos Inc., 1699 South Hanley Rd., St. Louis, Missouri 63144, USA.
[28] C. I. Bayly, P. Cieplak, W. D. Cornell, P. A. Kollman, *J. Phys. Chem.* **1993**, *97*, 10269–10280.
[29] H. J. C. Berendsen, J. P. M. Postma, W. F. Van Gunsteren, A. Di Nola, J. R. Haak, *J. Chem. Phys.* **1984**, *81*, 3684–3690.

Received: October 17, 2003
Revised: December 12, 2003 [F5633]